ASN NEURO RESEARCH ARTICLE

ASN NEURO 2(4):art:e00043.doi:10.1042/AN20100016

Increased *Plp1* gene expression leads to massive microglial cell activation and inflammation throughout the brain

Carrie L Tatar*, Sunita Appikatla*, Denise A Bessert*, Ajaib S Paintlia†, Inderjit Singh† and Robert P Skoff*[1]
*Department of Anatomy and Cell Biology, Wayne State University, Detroit, MI 48201, U.S.A.
†Department of Pediatrics, Medical University of South Carolina, Charleston, SC 29425, U.S.A.

Cite this article as: Tatar CA, Appikatla S, Bessert DA, Paintlia AS, Singh I and Skoff RP (2010) Increased *Plp1* gene expression leads to massive microglial cell activation and inflammation throughout the brain. ASN NEURO 2(4):art:e00043.doi:10.1042/AN20100016

ABSTRACT

PMD (Pelizaeus–Merzbacher disease) is a rare neurodegenerative disorder that impairs motor and cognitive functions and is associated with a shortened lifespan. The cause of PMD is mutations of the *PLP1* [proteolipid protein 1 gene (human)] gene. Transgenic mice with increased *Plp1* [proteolipid protein 1 gene (non-human)] copy number model most aspects of PMD patients with duplications. Hypomyelination and demyelination are believed to cause the neurological abnormalities in mammals with *PLP1* duplications. We show, for the first time, intense microglial reactivity throughout the grey and white matter of a transgenic mouse line with increased copy number of the native *Plp1* gene. Activated microglia in the white and grey matter of transgenic mice are found as early as postnatal day 7, before myelin commences in normal cerebra. This finding indicates that degeneration of myelin does not cause the microglial response. Microglial numbers are doubled due to *in situ* proliferation. Compared with the jp (jimpy) mouse, which has much more oligodendrocyte death and hardly any myelin, microglia in the overexpressors show a more dramatic microglial reactivity than jp, especially in the grey matter. Predictably, many classical markers of an inflammatory response, including TNF-α (tumour necrosis factor-α) and IL-6, are significantly upregulated manyfold. Because inflammation is believed to contribute to axonal degeneration in multiple sclerosis and other neurodegenerative diseases, inflammation in mammals with increased *Plp1* gene dosage may also contribute to axonal degeneration described in patients and rodents with *PLP1* increased gene dosage.

Key words: inflammation, microglia, myelin, Pelizaeus–Merzbacher disease, proteolipid protein, oligodendrocyte.

INTRODUCTION

PMD (Pelizaeus–Merzbacher disease) is an X-linked neurodegenerative disorder of the CNS (central nervous system) caused by missense mutations, duplications and deletions of the *PLP1* [proteolipid protein 1 gene (human)] gene. Duplications/triplications of the native *PLP1* gene are most frequent, accounting for nearly 70% of males that have PMD (Garbern et al., 1999). Clinically, nystagmus, psychomotor developmental delay, spasticity, hypotonia and ataxia present within the first 2 months of life in connatal forms of the disease (Hodes et al., 1993). Investigators have concluded that a major biological function of PLP protein is to maintain the structural integrity of the myelin sheath (Duncan et al., 1987; Boison et al., 1995). However, the protein has other functions that include regulation of oligodendrocyte cell death (Knapp, 1996; Yang and Skoff, 1997; Nadon and West, 1998; Cerghet et al., 2001). There are currently no cures or treatment options available for this rare disease, and the cellular and molecular mechanisms that lead to the phenotypes are poorly understood.

Transgenic rodents with *Plp1* [proteolipid protein 1 gene (non-human)] increased gene dosage are valid models for PMD because they show the same behavioral deficits that include a shortened lifespan as PMD patients (Mastronardi et al., 1993; Kagawa et al., 1994; Readhead et al., 1994; Bradl et al., 1999). At the cellular level, many different abnormalities have been described in *Plp1* transgenics that include not only defects in

[1]To whom correspondence should be addressed (email rskoff@med.wayne.edu).
Abbreviations: BrdU, bromodeoxyuridine; CCL3, CC chemokine ligand 3; CCR1, CC chemokine receptor 1; CD8, cluster of differentiation 8; CD11b, cluster of differentiation molecule 11B; CNS, central nervous system; CRP, C-reactive protein; CXCL, CXC chemokine ligand; DAB, diaminobenzidine; DPN, day postnatal; EAE, experimental allergic encephalomyelitis; GAPDH, glyceraldehyde-3-phosphate dehydrogenase; HRP, horseradish peroxidase; Iba1, ionized calcium-binding adaptor molecule 1; IL-1β, interleukin-1β; iNOS, inducible nitric oxide synthase; jp, jimpy; MOG, myelin oligodendrocyte glycoprotein; PMD, Pelizaeus–Merzbacher disease; *PLP1*, proteolipid protein 1 gene (human); *Plp1*, proteolipid protein 1 gene (non-human); QPCR, quantitative PCR; qRT–PCR, quantitative reverse transcription–PCR; Ta, Tabby; TNF-α, tumour necrosis factor-α.

oligodendrocytes but also neurons. Mice with *Plp1* increased gene dosage exhibit major oxidative phosphorylation defects that include 50% reductions in ATP brain levels and decreased mitochondrial membrane potentials in neurons as well as oligodendrocytes (Hüttemann et al., 2009). Axonal degeneration is also a peculiar feature of rodents that overexpress the *Plp1* gene (Anderson et al., 1998; Griffiths et al., 1998). However, the sequence of events that begins with increased *Plp1* gene transcription and leads to axonal degeneration is unknown. In the present study, we describe microglial activation and up-regulation of pro-inflammatory cytokines in the cerebrum of a transgenic mouse that overexpresses native *Plp1* (*Plp1*tg). The relevance of an inflammatory response cannot be underestimated because inflammation is a known major contributor to axonal damage and subsequent neurological sequelae in many neurodegenerative diseases.

Microglial cells are considered resident macrophages of the CNS that act as immune defence cells. In normal mature brains, microglial cells are responsible for immune surveillance (Block and Hong, 2005) and exhibit a distinctive morphology in normal mammals. Microglia can also become activated and turn into motile, amoeboid cells and play a major role in initiation and progression of neurodegenerative diseases (Dickson et al., 1991; Thomas, 1992; McGeer et al., 1993; Kreutzberg, 1996; Gonzalez-Scarano and Baltuch, 1999). These cells undergo dramatic morphological alterations upon brain injury or immunological stimuli transforming from resting microglia into activated amoeboid microglia (Kreutzberg, 1996). For example, in the demyelinating disorder multiple sclerosis, microglia proliferate and increase lysosomal activity around active sites of demyelination (Matsumoto et al., 1992).

This is the first study that shows microglial activation in a transgenic mouse that overexpresses native *Plp1*. Microglial activation in the spinal cord of the jp (jimpy) mouse, a mouse with a *Plp1* missense mutation, characterized by its severe hypomyelination has been described (Vela et al., 1995). The optic nerve and spinal cord of *Plp1*tg mice are characterized by demyelination, but the striatum and cortex are surprisingly normal (Readhead et al., 1994). Therefore it would not be expected that microglia exhibit intense reactivity in areas of the cerebrum if microglial activation is based solely on hypomyelination/demyelination. To our surprise, we found that microglial activation begins before myelination commences in the normal cerebrum. Accordingly, interactions between oligodendrocytes and axons rather than frank demyelination and/or hypomyelination must lead to axonal degeneration (Garbern et al., 2002). Thus strategies to modulate oligodendrocyte function *in vivo* are necessary to alter the course of PMD if myelin abnormalities are not the direct cause of certain debilitating diseases (Garbern et al., 2002).

To support the hypothesis that an immune response is occurring in *Plp1*tg mice, we found extensive microglial activation accompanied by an increase in many cytokines that are also elevated in CNS disorders. For example, TNF-α (tumour necrosis factor-α) and IL-6 (interleukin-6) are elevated in several CNS disorders (Navikas and Link, 1996; Vladic et al., 2002; Baraczka et al., 2004). Recent studies demonstrate that TNF-α exacerbates focal ischaemic brain injury and that blocking endogenous TNF-α is neuroprotective (Barone et al., 1997). What role these cytokines play in exacerbating oligodendrocytes and neuronal dystrophies in animals with *Plp1* increased gene dosage is yet to be determined.

MATERIALS AND METHODS

Animals

Male and female 7, 19–27, 50 and 70 DPN (day postnatal) B6CBA mice (Jackson Laboratory, Bar Harbor, ME, U.S.A.) and male and female *Plp1*tg mice (Readhead et al., 1994) were used for genotyping, immunocytochemistry, cytokine assays and electron microscopy. *Plp1*tg mice aged 30 days and older were first identified by tremors and seizures followed by extraction of DNA from tails with the Qiagen DNA easy kit (Qiagen, Valencia, CA, U.S.A.). DNA from both tremoring *Plp1*tg mice and presumptive *Plp1*tg mice younger than 30 days were used to measure copy number. Copy number was calculated with the $\Delta\Delta C_t$ (C_t is threshold cycle value) method using a wild-type male with one *Plp1* gene as the calibrator (Regis et al., 2005). *Plp1*tg mice that had at least two extra copies of the native *Plp1* gene and exhibited tremors and seizures were studied. QPCR (quantitative PCR) was performed with an Eppendorf Realplex PCR system using SYBR Green (Stratagene, La Jolla, CA, U.S.A.). Seventeen–19 DPN jp mice (jp+/+Ta; Ta is tabby) were obtained from our breeding colony housed in the Division of Laboratory Animal Resources, a federally approved animal facility. *Plp1*/jp/Ta female carriers (jp+/+Ta) and males (+Ta) were purchased from Jackson Laboratory. jp mice at 17–19 DPN were identified by tremors and seizures and then genotyped by PCR following the procedure in Hüttemann et al. (2009). All mice were housed in DLAR animal facilities that are under the direct supervision of IACUC, a federally approved institutional committee; all procedures were approved by the Wayne State University IACUC.

Immunocytochemistry

Mice were anaesthetized with an intraperitoneal lethal dose of chloral hydrate. All animals were perfused intracardially with 4% (w/v) paraformaldehyde and their brains were removed and placed in buffer. Then, 50 μm sections were cut with a Vibratome, washed with PBS, treated with 10% Triton for 1 h, treated with 3% H_2O_2 for 25 min, blocked with 10% (v/v) goat serum for 30 min, and incubated in polyclonal anti-Iba1 (ionized calcium-binding adaptor molecule 1) antibody (Wako, Richmond, VA, U.S.A.) diluted 1:500 overnight in 0.1 M

PBS at room temperature (20°C). The next day, sections were rinsed in PBS and incubated in goat anti-rabbit IgG HRP (horseradish peroxidase; Jackson ImmunoResearch)-conjugated antibody diluted 1:100 and detected using 0.5 mg/ml DAB (diaminobenzidine) without or with 0.2 mg/ml cobalt chloride (Sigma–Aldrich, St. Louis, MO, U.S.A.).

For combined Iba1 and BrdU (bromodeoxyuridine) immunostaining of 8 DPN mice, mice were injected with 100 μg of BrdU/g of body weight intraperitoneally and perfused with 4% paraformaldehyde 40 h later. The interval from injection to sacrifice permits microglia/microglial precursors to divide and differentiate. Then, 50 μm sections were cut with a Vibratome, washed in PBS, treated with 2 M HCl for 30 min at 37°C, incubated in 0.1 M sodium borate twice for 30 min at room temperature, treated with 3% H_2O_2, incubated in PBS-blocking buffer (PBS containing 0.2% BSA, 0.2% milk and 1.0% Triton) for 30 min and incubated with anti-BrdU (BD Biosciences, San Jose, CA, U.S.A.) diluted 1:100 at 4°C overnight. Sections were rinsed in PBS, incubated in anti-mouse HRP (Jackson ImmunoResearch) conjugated and developed with DAB. Sections were then rinsed in PBS and processed for Iba1 immunocytochemistry as previously described and developed using DAB without cobalt.

An F4/80 antibody (Jackson ImmunoResearch) was used to detect macrophages in 3 months *Plp1*tg cervical spinal cords. Then 50 μm sections (prepared as described above) were rinsed in PBS, treated with 3% H_2O_2 for 20 min, blocked with 10% goat serum for 1 h and incubated in polyclonal anti-F4/80 antibody diluted 1:100 overnight in 0.1 M PBS at 4°C. The next day, sections were rinsed in PBS and incubated in goat anti-rat IgG HRP-conjugated antibody (Jackson ImmunoResearch) diluted 1:100 and detected using 0.5 mg/ml DAB (Sigma–Aldrich). As a positive control, spinal cord sections from EAE (experimental allergic encephalomyelitis) mice injected with MOG (myelin oligodendrocyte glycoprotein) were stained alongside *Plp1*tg sections.

Quantification of microglia

Microglia in the cortex and striatum of *Plp1*tg 19–27 DPN and B6CBA 23–27 DPN brain sections were counted using a Leitz (Wetzlar, Germany) Laborlux microscope. Only cobalt enhanced sections were used for counting. Cells were counted with a $\times 50$ oil objective and a $\times 10$ eyepiece containing a 1 cm^2 grid divided into 1 mm squares. The grid was placed over the dorsal cortex, immediately superior to the corpus callosum and adjacent to the interhemispheric sulcus, the ventral–lateral cortex, adjacent to the most ventral tip of the corpus callosum, and the striatum, immediately inferior to the corpus callosum and adjacent to the lateral ventricle (Figure 6). For each animal, three matched transverse sections at the level of the anterior commissure were used. The number of cells for each area was summed and the averages determined. Microglia were only counted if the nuclear membrane was completely intact as visualized by focusing completely through the section.

Plastic embedded tissue

Animals were perfused intracardially with 4% paraformaldehyde and 0.5% glutaraldehyde. Cerebra were dissected and 200 μm thick sections were embedded in Araldite plastic following routine laboratory procedures (Bessert and Skoff, 1999). Semi-thin sections (1 micron) were stained with Toluidine Blue. Ultrathin sections were cut, stained with uranyl acetate and lead citrate and examined with a Jeol 1010 transmission electron microscope. Negatives were scanned at 1600 dpi (dots per inch) using Adobe Photoshop.

Mouse inflammatory cytokines and receptors PCR array

The Mouse Inflammatory Cytokines and Receptors RT^2 Profiler™ PCR Array (SABiosciences, Frederick, MD, U.S.A.) that profiles the expression of 84 key genes involved in a focused inflammatory pathway was run to screen for inflammation in a *Plp1*tg mouse. Total RNA was isolated from the brain of a *Plp1*tg mouse and a C57BL/6 control at 27 DPN using TRIzol® reagent (Invitrogen). RNA was purified using RNeasy® Min Elute™ cleanup columns (Qiagen). RNA (0.5–1 μg) from each sample was used to synthesize the reverse transcriptase (cDNA) first strand following the instructions of RetroScript (Ambion, CA, U.S.A.). The cDNA is used as a template in the RT profiler™ PCR Super Array, and QPCR was performed following a two-step cycling programme on Eppendorf Mastercycler® Eppendorf Realplex. The fold change in gene expression was calculated using the $\Delta\Delta C_t$ Data Analysis Method; the *Plp1*tg mouse used had four copies of the *Plp1* gene and showed tremors and seizures.

Quantitative real-time PCR analysis of cytokines and chemokines

CCL3 (CC chemokine ligand 3), CCL8 (CC chemokine ligand 8) and CRP (C-reactive protein) (Table 1) were determined by QPCR. Reverse transcriptase was obtained as described above and the reverse transcript was subjected to real-time PCR on the Eppendorf Mastercycler® Eppendorf Realplex in the presence of SYBR Green I dye (Stratagene). A two-step QPCR was performed for 40 cycles (10 min at 95°C, 15 s at 95°C and 1 min at 60°C). Product identity was confirmed by melting point analysis. GAPDH (glyceraldehyde-3-phosphate dehydrogenase) served as an internal reference gene in all the experiments. Real-time PCR was performed in triplicates for both the target gene and GAPDH. The level of gene expression was calculated after normalizing against GAPDH in each sample and is presented as relative mRNA expression. The total cDNA subjected to amplification was calculated using the $\Delta\Delta C_t$ method.

Table 1 List of primers used in QPCR analysis

Gene (accession number)	Forward primer	Reverse primer
CCL3 (NM011337)	5′-AGACCTGGTCCAAGAAGAATACAT-3′	5′-CTCAAGCCCTGCTCTACAC-3′
CCL8 (NM021443)	5′-CAGACCAAGCAGGGTATGTC-3′	5′-TCTCTGCCTGGAGAAGATTAGG-3′
CRP (NM007768)	5′-TCAGGACAGCCACTGATTACCTC-3′	5′-TAGGTTGCCCAAACAAGACC-3′
TNF-α (NM11731)	5′-AGCCGATGGGTGTACCTTGTCTA-3′	5′-TGAGATAGCAAATCGGCTGACGGT-3′
IL1-β (NM15131)	5′-TGGAGAGTGTGGATCCCAAGCAAT-3′	5′-TGCTTGTGAGGTGCTGATGTACCA-3′
IL-6 (J03783)	5′-TGGCTAAGGACCAAGACCATCCAA-3′	5′-AACGCACTAGGTTTGCCGAGTAGA-3′
iNOS (BC027514)	5′-GTGGCTTCTTCTACACACCCATGT-3′	5′-GCACTGATCTACAATGCCACGCTT-3′

RESULTS

Microglial morphology of *Plp1*tg compared with B6CBA mice

Iba1 is a polyclonal antibody that recognizes an ionized calcium-binding adaptor molecule that is only expressed in microglia in the brain (Imai et al., 1996; Graeber et al., 1998; Ito et al., 1998). This antibody has been used to identify microglia in many mammalian species (Tonchev et al., 2003; Yamada et al., 2006). Iba1 immunostained microglial cells are present throughout the grey and white matter of both the normal B6CBA and the *Plp1*tg mouse cerebrum (Figure 1). Typical microglia in normal cerebra, often referred to as ramified, have characteristic long and thin processes of even calibre (Figure 1A). Their primary processes are usually twice as long as the long axis of the perikaryon. Secondary processes branch acutely from primary processes, and sometimes tertiary processes are distinguishable. Perikarya are characteristically oval-, pear- or triangular-shaped and are easily distinguished from the smoothly contoured round oligodendroglia perikarya and the larger, irregularly shaped astroglial perikarya. The ramified morphology is similar across all age groups that we studied in normal B6CBA mice.

Low-magnification pictures show that the distribution of microglia in normal cerebra is evenly spaced, with minimal contact between processes of neighbour microglia in both the cortex (Figure 1B), striatum (Figure 1C) and corpus callosum (Figure 1D).

In the *Plp1*tg mice, the morphology and dispersion of these cells in the cortical, striatal and callosal regions of cerebra drastically differ from the B6CBA controls (Figures 2A and 2B) in all age groups analysed (Figures 2C–2F). Activated microglia in all *Plp1*tg age groups are distinguished by coarse and short processes, a notable increase in the amount of these processes, and an enlargement of the cell body within the cortical (Figures 2C and 2E) and striatal (Figures 2D and 2F) regions. In the cortices, microglia are often clustered together with an entanglement of brush-like processes. This arrangement has been previously described and is due to actively proliferating microglia cells as an early response to neurodegeneration (Dissing-Olesen et al., 2007). This pattern is most easily observed between the cortex and the white matter in the ventral cortex. In the striatum, microglial processes run parallel with each other with long straight processes, as if they are following axonal trajectories.

Corpora callosa of normal B6CBA mice appear to have fewer microglia than grey matter (Figure 1D). When compared with controls (Figures 1, 2A and 2B), white matter in *Plp1*tg have an abundance of activated microglia (Figures 3A–3C), with coarse, straight processes that parallel the trajectory of callosal axons.

Microglial morphology of *Plp1*tg mice changes as the mice age

With age, the activation of microglia increases in the *Plp1*tg cerebra. In the cortices and striata at 30 DPN (Figures 2E and 2F), microglia have stubby processes and are found in clusters with other brush-like microglia. At 19 DPN (Figures 2C and 2D), the transition from a ramified morphology to a reactive morphology is noticeable as processes shorten in length and diameter. In the striatum at 19 DPN (Figure 2D), cell processes do not follow a particular path as do the 30 DPN (Figure 2F) processes.

In both white and grey matter at 7 DPN, the earliest age studied, activation of microglia has already begun in the *Plp1*tg cerebra (Figures 4C–4E). While many microglia have a normal morphology, others exhibit shortened and numerous processes. Individual microglia appear to have long, thin processes typical of ramified microglia on one side of the cell and shortened, numerous processes typical of reactive microglia at the opposite side of the cell. Microglia in normal brains at this age (Figures 4A and 4B) are similar to microglia at older ages, having long processes that often end in an expanded ball. At 7 DPN in the normal brain, myelinated fibres are not yet detectable in 1 µm plastic sections (Figure 4F). Myelinated axons have dark rings surrounding an opaque centre and easily visible in semi-thin plastic sections. Therefore the activation of microglia at this age is not due to abnormal myelin structure or demyelination.

Generation of new microglia in 8 DPN *Plp1*tg mice

In addition to microglia activation beginning at 7DPN, microglia are stimulated to divide at this young age. Combined Iba1 and BrdU immunostaining was performed on *Plp1*tg cerebra with two or more copies of *Plp1*. Mice were injected intraperitoneally with BrdU on 6 DPN and killed 40 h later on 8 DPN. Generation of new microglia is abundant because $Iba1^{+}/BrdU^{+}$ microglia are present in the cerebrum (Figures 5A–5D). Microglia in the metaphase stage of mitosis (Figure 5B) have been detected, indicating that microglia

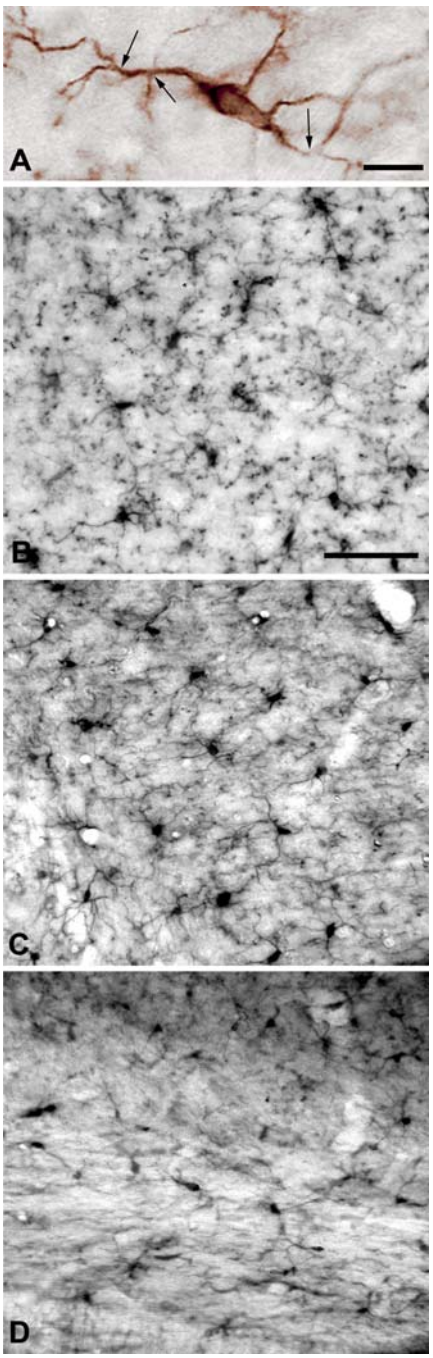

Figure 1 Iba1 immunostaining of 50 μm Vibratomed sections from 36–46-day-old normal B6CBA mouse cerebra visualized with DAB alone (A) or cobalt-enhanced after DAB development (B–D)

High magnification of a typical ramified microglial cell (**A**) shows several long, thin processes emanating from an ellipsoid cell body. These primary processes branch into secondary processes (arrows). In areas of the cortex (**B**) and striatum (**C**), resting microglia are evenly dispersed throughout grey matter with typical ramified morphology. In the corpus callosum (**D**), microglia are less abundant than in grey matter, but retain their ramified morphology. The cingulum is at the top of the Figure. Scale bars: (**A**) 10 μm and (**B–D**) 50 μm.

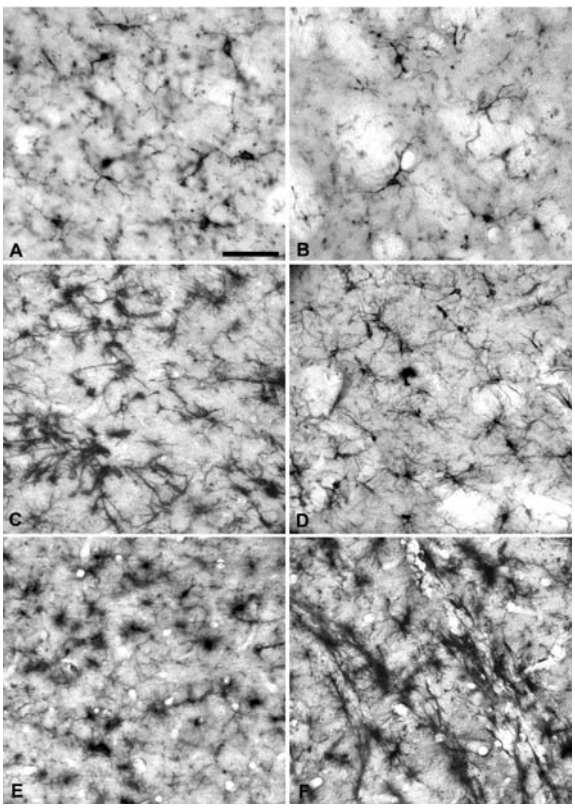

Figure 2 Iba1 cobalt-enhanced immunostaining of 50 μm Vibratomed sections from a 50-day-old B6CBA cortex (A) and striatum (B) and *Plp1*tg cortex (C, E) and striatum (D, F) of 19DPN (C, D) and 30DPN (E, F) transgenics

Microglia from B6CBA mice at 50 DPN have similar morphology to microglia at younger ages. Activated microglia are often clustered together with their cell bodies having a fuzzy appearance due to numerous, short, thick processes. In the striatum, more elongated and straighter processes are visible, possibly following axonal trajectories. Microglia exhibit more processes at 30 DPN (**E**, **F**) than at earlier ages (**C**, **D**). Scale bar, 50 μm.

divided approx. 40 h earlier at the time of the BrdU injection and shortly before killing. Figure 5 also shows many $BrdU^+$ cells that are not $Iba1^+$; these cells serve as a control to show that the BrdU-labelled cells are not non-specifically labelled with the Iba1 antibody. Some of these $BrdU^+$ cells are $Olig1^+$, indicating that oligodendrocyte progenitors are stimulated to divide (results not shown).

The number of microglia is increased in *Plp1*tg mice

*Plp1*tg mice with increased gene dosage lead to an increase in microglia cell number in both white and grey matter of the cerebrum when compared with B6CBA mice. A low-magnification micrograph (Figure 6A) shows a hemi-section at the level of the anterior commissure at 30 DPN of the mice. For quantification, only cobalt-enhanced sections were used for both control and *Plp1*tgs. The number of $Iba1^+$ microglial cells was counted directly through the microscope with a $\times 50$ oil objective and a $\times 10$ eyepiece (see the Materials and

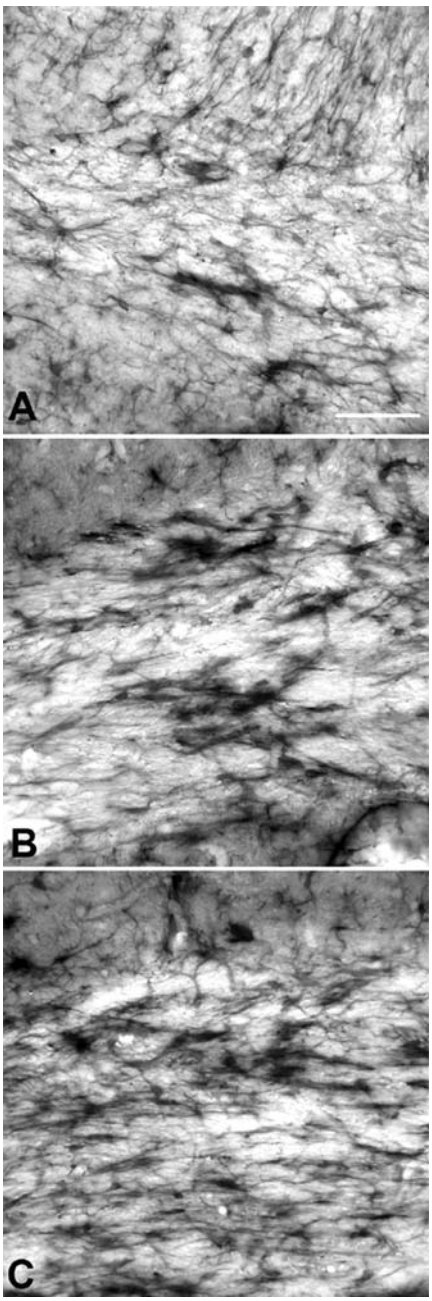

Figure 3 Iba1 cobalt-enhanced immunostaining of 50 μm Vibratomed sections from the corpus callosum of 19- (A), 30- (B) and 50-day-old (C) *Plp1*tg mice display activated microglia, where processes follow trajectories of callosal axons
At 30 and 50 DPN, microglia are more activated in the white matter compared with the 19 DPN. Scale bar, 50 μm.

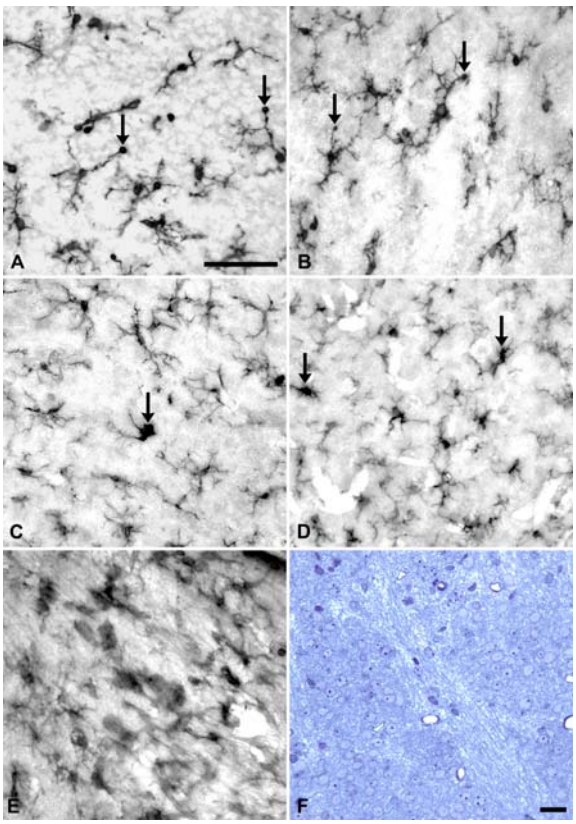

Figure 4 Iba1 cobalt-enhanced immunostaining of 50 μm Vibratomed sections from 7 DPN B6CBA (A, B) and *Plp1*tg mice (C–E)
Microglia in the cortices (**A**) and striatum (**B**) of normal mice already display the characteristic morphology of microglia at older ages. Their long processes sometimes terminate in boutons (arrows) that are less prominent in microglia from older mice. In the cortex (**C**), striatum (**D**) and corpus callosum (**E**), some microglial cells in *Plp1*tg mice are already activated at this young age, indicated by short, numerous processes emanating from microglia with large perikarya (arrows). Note the absence of long processes on some of these activated microglia. A mix of ramified and activated microglial cells is visible in all three regions. (**F**) A 1 μm plastic section of a normal 7 DPN B6CBA striatum has no myelin around axons at this age. Scale bars: (**A–E**) 50 μm and (**F**) 10 μm.

methods section). It can be seen that 19–27-day-old *Plp1*tg have significant increases ($P<0.0001$; Figure 6B) in all three areas counted: dorsal cortex immediately superior to the corpus callosum and adjacent to the inter-hemispheric sulcus, the ventral–lateral cortex adjacent to the most ventral tip of the corpus callosum, and the striatum immediately inferior to the corpus callosum and adjacent to the lateral ventricle. The results indicate that the density of microglia cells is higher in *Plp1*tgs (Figure 6B), with a 76% increase in the dorsal cortex, a 95% increase in the ventral–lateral cortex and 85% increase in the striatum. It is likely that the increase in microglia in *Plp1*tg mice is even greater than the cell counts because microglia are clustered together and sometimes it is difficult to determine the exact number.

Ultrastructure of microglia

Microglia in *Plp1*tg mice (Figures 7A and 7B) exhibit the same nuclear and cytoplasmic features as ramified microglia in normal mice. The chromatin forms a dense layer immediately beneath the nuclear membrane and the density of the cytoplasm is intermediate to that of oligodendrocytes and astrocytes (Skoff, 1975). However, the activated microglia in

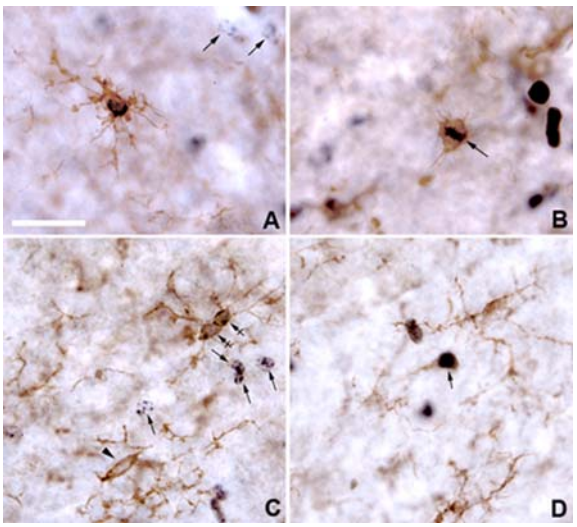

Figure 5 Combined Iba1 and BrdU immunostaining of 50 μm Vibratomed sections from a 8 DPN *Plp1*1tg mouse

Mice were injected with BrdU at 6 DPN and killed 40 h later on 8 DPN. Brown chromogen indicates Iba1 cytoplasmic staining and black chromagen indicates BrdU nuclear staining. (**A**) A double-labelled microglia cell with numerous processes indicates that this cell underwent cell division approx. 40 h before the mouse was killed. Two $BrdU^{+}/Iba1^{-}$ cells (arrows) are shown in the upper right. (**B**) An $Iba1^{+}$ cell that is in mitosis (arrow). (**C**) Four $BrdU^{+}/Iba1^{-}$ cells (arrows), a $BrdU^{-}/Iba1^{+}$ cell (arrowhead) and a pair of lightly labelled $Brdu^{+}/Iba1^{+}$ cells (crossed arrows). (**D**) A double-labelled microglial cell with one process (arrow). Scale bar, 50 μm.

*Plp1*tg mice often contain degenerating material of unknown origin. They tend to have larger perikarya and thicker processes than ramified microglia. These features probably correspond to the larger cell body and thick coarse processes visualized with Iba1 immunostaining. In addition to the activated microglia present in *Plp1*tg, small, dark cells are also occasionally present (Figures 7C and 7D). These cells have too little cytoplasm to permit definitive classification. The cell in Figure7(C) has the nuclear features of an oligodendrocyte progenitor; the cell in Figure 7(D) has the nuclear features of a microglial cell or oligodendrocyte as these cell types often directly abut the perikarya of neuronal somata. Conversely, they may be immune cells that have invaded the CNS.

Microglial response in jp mice

jp mice have a missense mutation in the *Plp1* gene, and they exhibit an intense astrocytic hypertrophy and hyperplasia that accompanies the virtual lack of myelin (Skoff, 1976). In contrast with the *Plp1*tg mice, microglial reactivity in jp is restricted mainly to the white matter (Figures 8A and 8B). Furthermore, the Iba1 immunostaining in jp does not appear to be as intense as in the *Plp1*tgs.

Up-regulation of cytokines

Based on the intense reactivity of microglia in *Plp1*tg mice, we predicted the up-regulation of classical inflammatory markers. qRT–PCR (quantitative reverse transcription–PCR)

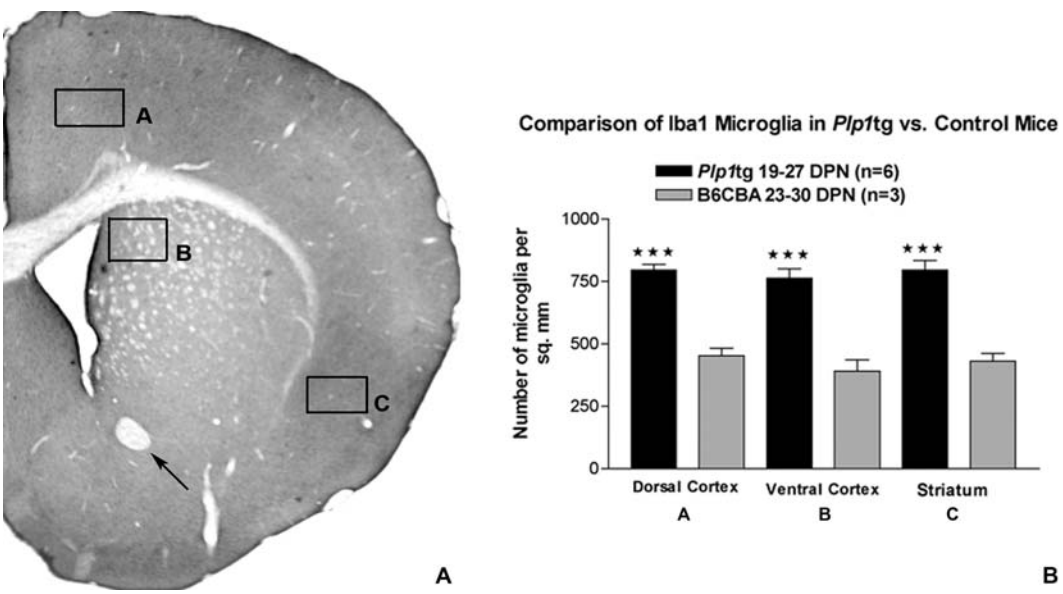

Figure 6 Quantification of microglia in *Plp1*tg versus control mice

(**A**) A 50 μm Vibratomed hemi-section from a 30 DPN mouse cerebrum at low magnification shows boxed areas used for quantification of Iba1 immunostained cells. Cells were counted at × 500 directly under the microscope at the level of the anterior commissure (arrow). Microglial cells with distinct nuclei were counted in the three areas selected: (**A**) dorsal cortex, (**B**) striatum and (**C**) ventral–lateral cortex. (**B**) Quantification of Iba1-immunostained cells in the cerebrum of 19–27 DPN *Plp1*tg and 23–30 DPN B6CBA mice. Values are means ± S.E.M. for Iba1 cells in the three areas selected, three sections per animal were averaged, and the number of animals from both groups is shown in parentheses. The two-tailed Student's *t* test was used to compare *Plp1*1tg mice with B6CBA mice; ***$P<0.0001$.

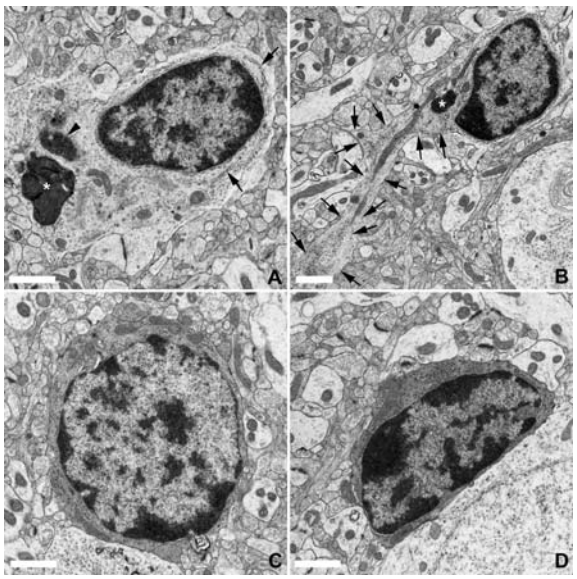

Figure 7 Ultrastructure of microglia in *Plp1*tg mice
(**A–D**) Electron micrographs from a 43 DPN *Plp1*tg mouse. (**A**) This typical microglial cell is characterized by dense heterochromatin lining the nuclear membrane. Contrasting light cytoplasm is typical of microglia, whereas oligodendrocytes have much more electron-dense cytoplasm. Long, thin strands of endoplasmic reticulum (arrows) with scattered ribosomes on their surface are likewise a distinguishing feature of microglia. A large inclusion (asterisk), as well as the remnants of an engulfed nucleus (arrowhead), is present in the cytoplasm. (**B**) A microglial cell with a long, thickened process (arrows) contains debris (asterisk). The large diameter process probably corresponds to the thickened processes seen in light micrographs. (**C**) An electron-dense cell with sparse cytoplasm lacks sufficient nuclear and cytoplasm features for positive identification. (**D**) Another electron-dense cell that is difficult to identify. This electron-dense cell abuts the perikaryon of a neuron, and these are characteristics of perineuronal oligodendrocytes. Scale bar, 1 μm.

expression of different inflammatory markers showed significant increases in two classical inflammatory markers, TNF-α and IL-6; they were significantly increased by 24- and 7-fold respectively at 7–8 weeks after birth compared with controls (Table 2). However, there was no increase in IL-1β or iNOS (inducible nitric oxide synthase) at 7–8 weeks of age. Based on a Mouse Inflammatory Cytokine and Receptor RT^2 Profiler^{TM} (SABiosciences) that profiles the expression of 84 key genes, we selected the chemokines CCL3, CCL8 and inflammatory marker CRP for qRT–PCR. Expression of CCL8 was significantly increased by 3.5-fold at 3 weeks and then significantly increased by 15-fold by 8 weeks postnatal. Expression of CCL3 was increased by 4-fold at 3 weeks and only slightly increased by 4.8-fold at 8 weeks postnatal. Similarly, CRP increased modestly from 3 to 8 weeks postnatal compared with normal mice. These results indicate that activation of inflammatory markers is well advanced by 3 weeks of age, and even increases for some markers as the disease progresses.

The qRT–PCR data shown above confirm the results of a cytokine and receptor Super Array profile performed on a *Plp1*tg and a wild-type mice at 27 DPN that showed similar increases in message levels for these chemokines (Table 3).

The cell types expressing these inflammatory markers and their receptors are unknown but are likely to involve a combination of macroglia, microglia and, possibly, immune cells because markers of T and B immune cells have been detected in the *Plp1*tg mice (Ip et al., 2006). We investigated whether macrophages invaded the CNS in the *Plp1*tg mice. The F4/80 surface antigen was easily detected in spinal cord sections of C57BL/6 mice with EAE injected with MOG-(35–55) (Figure 9A). However, spinal cord sections from *Plp1*tg mice processed alongside the EAE sections showed non-specific staining, mainly in axons (Figure 9B). The picture shown here represents the most intense staining we found in the overexpressors.

DISCUSSION

The coding region of the *PLP1* gene in humans is identical with the *Plp1* gene at the amino acid level in rodents (e.g. Stoffel et al., 1985; Macklin et al., 1987), suggesting that the same mutations in rodents as in humans might exhibit the same cellular abnormalities and behavioural deficits. Indeed, increased gene dosage of the *PLP1* gene in humans and *Plp1* gene in transgenic rodents exhibit many similar behavioural abnormalities that include ataxia, tremors and often a shortened lifespan (Garbern et al., 1999). At the tissue level, both rodents and humans with increased gene dosage exhibit demyelination and/or hypomyelination. At the cellular level, death of oligodendrocytes and axonal degeneration have been described in humans and in rodents with higher copy number (Gow et al., 1998; Griffiths et al., 1998; Anderson et al., 1999; Cerghet et al., 2001; Skoff et al., 2004a, 2004b). The molecular and cellular sequence of events that cause the tissue and behavioural abnormalities is poorly understood. Since PLP is expressed at high levels only in oligodendrocytes, it is generally assumed that oligodendrocytes and/or abnormal structure of myelin must directly cause all the abnormalities, including axonal degeneration. However, in many neurodegenerative diseases, secondary microglial activation and an inflammatory response have been described in many human diseases including Alzheimer's, Parkinson's and amyotrophic lateral sclerosis (Wojtera et al., 2005). In these neurodegenerative diseases, the contribution of microglia to inflammation and neuronal destruction is a subject of intense investigation. Hints that an inflammatory response was present in a human case of PMD have been described because a young male patient positively responded to corticosteroids (Gorman et al., 2007). In rodents with higher copy number, markers of immune and macrophage cells have been described (Ip et al., 2006; Edgar et al., 2010), but whether, and to what extent, inflammatory molecules are activated has not been examined.

Here, we describe for the first time intense microglial reactivity in *Plp1* transgenic mice and the up-regulation of

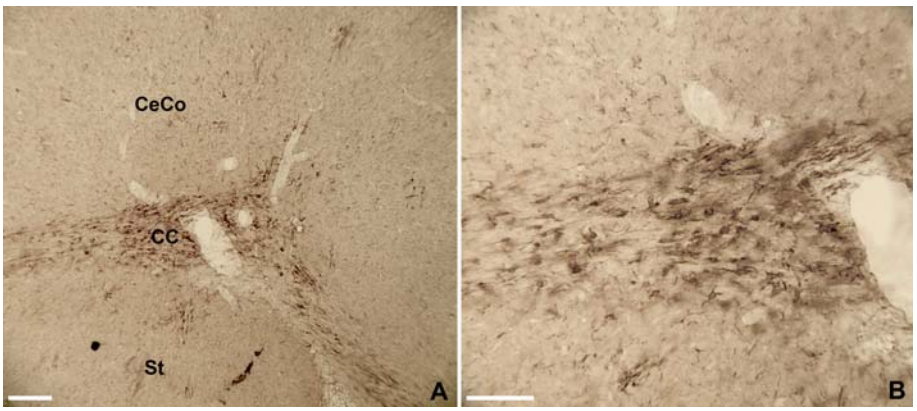

Figure 8 **Light micrographs of the brain from a 19 DPN jp mouse stained with Iba1 antibody**
(**A**) Microglial staining is strongest in corpus callosum (CC), but weak in cerebral cortex (CeCo) and striatum (St). Microglial staining in grey matter is limited to white matter bundles including cingulum in cortex and Combs fibres in striatum. (**B**) The microglia in jp corpus callosum do not exhibit the intense reactivity found in *Plp1*tg mice manifested by short, thick processes. Scale bar, 100 μm.

classical inflammatory markers. Although it remains to be determined whether and how the inflammation contributes to the neural degeneration in the *Plp1*tg mice, the well-known role of cytokine and chemokine activation in other neurodegenerative diseases makes it likely that microglial activation contributes to disease progression.

We find that increased *Plp1* gene dosage in line 66 of the *Plp1*tg mice (Readhead et al., 1994) leads to dramatic morphological changes of microglia. The morphological changes in microglia are as dramatic in the grey matter, if not more so, than in the white matter. From 3 weeks postnatal, shortening and thickening of microglial processes became progressively more pronounced in grey matter, and the number of microglial processes was increased. In the striatum and corpus callosum, microglial processes were increased, but they were longer and followed axonal trajectories. Whether they are interposed between oligodendrocyte processes and axons or directly abut axons is unclear. In active grey matter lesions in multiple sclerosis, activated microglia appose and ensheath apical dendrites, neurites and neuronal perikarya (Peterson et al., 2001). In the cerebral cortex in multiple sclerosis patients, more recent studies have demonstrated microglial activation associated with extensive demyelination (Bo et al., 2003; Kutzelnigg et al., 2005; Vercellino et al., 2005; Gray et al., 2008) but, more interestingly, microglial activation was noted in regions that are not demyelinated (Kutzelnigg et al., 2005). Following an experimentally induced axonal lesion in C57BL/6 mice, activated microglia were proliferating within 3 days and most of the proliferating microglia were aggregating into multicellular clusters (Dissing-Olesen et al., 2007), similar to that observed in our study. Previous studies have examined the distribution and morphology of microglia cells in diseased or injured spinal cord and noted greater microglia activation in white matter as opposed to grey matter (Vela et al., 1995; Vela et al., 1996; Zhang et al., 2008). In jp, the numbers of white matter microglia were 3–5-fold greater than in normal animals but only 60% greater in grey matter than normal animals . We found nearly a doubling of microglia in the grey matter of the *Plp1*tg mice and, as noted in the Results section, these numbers are likely to be underestimates because microglia are densely clustered together. These and our present study (see below) suggest that microglial activation is caused by other factors/molecules besides degeneration of myelin.

Most importantly, by the first postnatal week, transformation of resting microglia into activated microglia has begun in

Table 2 qRT–PCR analysis of mRNA expression of cytokines and chemokines in brain homogenates of *Plp1*tg mice
NS, not significant.

Inflammatory marker (number of animals)	Age (days)	Fold change of mRNA expression in *Plp1* compared with controls	Significance
CCL3 (3)	19–21	4.0	NS
CCL3 (5)	60	4.8	$P<0.05$
CCL8 (3)	19–21	3.5	$P<0.001$
CCL8 (5)	60	15.0	$P<0.02$
CRP (3)	19–21	3.5	$P<0.001$
CRP (5)	60	4.5	$P<0.05$
TNF-α (3)	50–60	23.7	$P<0.03$
IL-6 (3)	50–60	7.0	$P<0.03$
IL-1β (3)	50–60	0.8	NS
iNOS (3)	50–60	1.3	NS

Table 3 Overview of cytokine and chemokine mRNA expression in brain of *Plp1*tg mice (with >3-fold change)

Gene symbol	Description	Up- or down-regulated
CCL3	CC chemokine ligand 3	3.19
CCL4	CC chemokine ligand 4	8.02
CCL8	CC chemokine ligand 8	3.77
CCR1	CC chemokine receptor 1	3.02
CRP	C-reactive protein pentraxin-related	3.62
CXCL10	CXC chemokine ligand 10	5.29
CXCL9	CXC chemokine ligand 9	3.90
IL-4	Interleukin-4	3,28
IL-13	Interleukin-13	4.21
CCR6	CC chemokine receptor 6	−3.35
CXCL13	CXC chemokine ligand 13	−3.80
Spp1	Secreted phosphoprotein 1	−3.62

grey and white matter. Some microglia retain a normal morphology, whereas others are retracting and thickening their processes. The presence of myelin was examined in 1 μm plastic sections of complete transverse cerebral sections, in which individual myelinated axons can be resolved. At this age, axons are still unmyelinated in normal cerebrum. This observation demonstrates that microglial activation is neither due to demyelination nor due to hypomyelination. Of course, the primary cause of the microglial activation must be overexpression of the *Plp1* gene, but not necessarily defects in myelination. Both *Plp1* mRNA and the protein are detectable in mouse cerebra at this age (Macklin et al., 1991). While the principal function of PLP is often considered to be that of an adhesive molecule in myelin (Boison et al., 1995; Gudz et al., 2002), numerous studies show that PLP and DM20 have other functions (Nadon and West, 1998; Skoff and Knapp et al., 1990; Knapp et al., 1993; Campagnoni and Skoff, 2001) including regulation of cell death (Skoff et al., 2004a, 2004b). Recently, we described major oxidative phosphorylation defects in the *Plp1*tg mice that lead to 50% reduction of tissue ATP and loss of mitochondrial membrane potential. The cause of these metabolic defects is likely due to the insertion of PLP into mitochondria when the gene is overexpressed (Hüttemann et al., 2009). Activation of microglia by increases in extracellular or exogenous ATP has been described in numerous studies (Lambert et al., 2010; Gyoneva et al., 2009; Monif et al., 2009; Puthussery and Fletcher, 2009). Exogenous ATP, in turn, activates microglial purinergic receptors. However, as presented above, total ATP levels in tissue homogenates are reduced in these mice. The possibility that ATP or its degradation products are secreted into the extracellular space at higher-than-normal amounts by neuroglia is under investigation in our laboratory.

In *Plp1*tg mice, the number of $Iba1^+$ microglia is doubled by the third postnatal week, due to their endogenous proliferation. Injection of BrdU on 6 DPN and killing 40 h later on 8 DPN followed by Iba1 immunostaining show $BrdU^+$/$Iba1^+$ microglia with long, branching processes characteristic of resting microglia and microglia with short, slightly thickened processes characteristic of activated microglia. The cell proliferation studies, carried out between 6 and 8 DPN, lend further support to the hypothesis that microglial

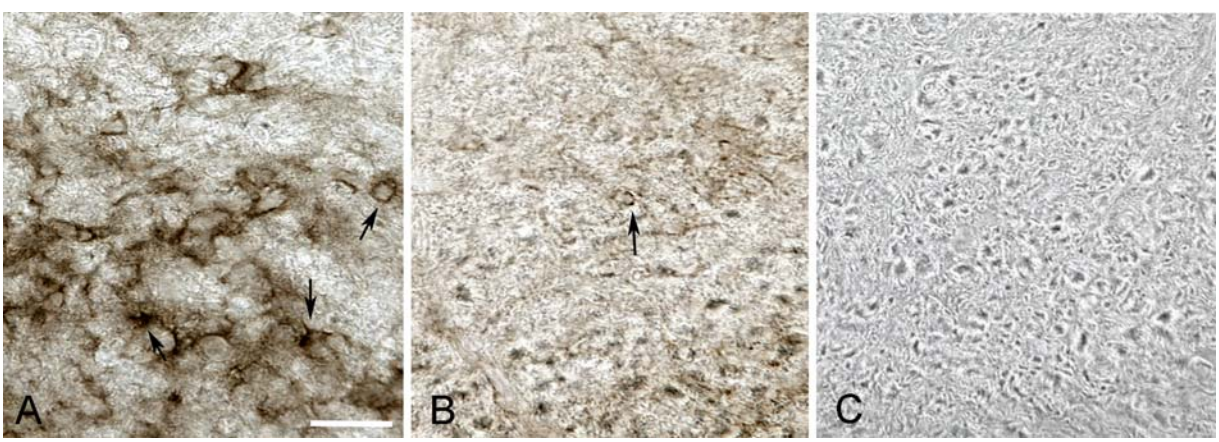

Figure 9 F4/80 immunostaining of 50 μm Vibratomed cervical spinal cords from an 8–9-month-old EAE mouse (A), a *Plp1*tg at 43 DPN (B), and the *Plp1*1tg without the F4/80 primary antibody (C)
(**A**) The EAE spinal cord shows macrophage infiltration (arrows) indicated by cytoplasmic and process staining of membranes. (**B**) The picture from the *Plp1*1tg ventral funiculus illustrates the most intense staining observed in these mutants. The axoplasm is non-specifically stained in these mutants. Scale bar, 5 μm.

activation is not due to demyelination/dysmyelination. Our findings agree with the data from jp mouse studies that show that endogenous microglia proliferate. In jp, activated microglial cells in the grey matter of the spinal cord were not associated with neurons, but were intermingled with nerve fibres crossing the grey matter laminae (Vela et al., 1995). The origin of additional microglia cells is unknown, but it is suggested that the main source of macrophage/reactive microglia cells in jp is the proliferation of endogenous microglial cells (Vela et al., 1995).

The intense microglial reactivity in *Plp1*tg mice suggests activation of multiple cytokines and chemokines. Not surprisingly, mRNA expression of classical inflammatory markers TNF-α and IL-6 were elevated 24- and 7-fold respectively in 2-month-old animals. Since TNF-α and IL-6 are activated by other regulatory molecules, we performed a multianalyte PCR analysis of inflammatory chemokines and their receptors from a 27 DPN *Plp1*tg mouse. mRNA levels of nine chemokines were elevated by more than 3-fold and several were down-regulated. For some of these chemokines such as CCL3/MIP-1α (macrophage inflammatory protein), its receptor (CCR1) is also up-regulated.

Many types of immune and glial cells secrete the chemokines and cytokines listed above. CCL3 and its receptor CCR1 have been identified on astrocytes, oligodendrocytes and radial glia after spinal cord injury (Knerlich-Lukoschus et al., 2010). CCL3 has also been identified in microglial cell lines of Sandhoff disease model mice (Kawashita et al., 2009). CRP, usually associated with susceptibility to stroke (Di Napoli et al., 2005), suppresses EAE, suggesting that it has a protective effect in this experimental model of multiple sclerosis (Szalai et al., 2002). CXCL13 (CXC chemokine ligand 13; BCA-1), a chemo-attractant for B lymphocytes, is down-regulated in these mice, suggesting that B-lymphocytes may not be attracted to the CNS. However, lymphocyte and macrophage markers ($CD8^+$ and $CD11b^+$) have been detected in aged heterozygous *Plp1*tg mice (Ip et al., 2006). We failed to find evidence of macrophages in the *Plp1*tg mice using the classical F4/80 antibody that we do not think is due to technical issues because in the same immunostaining experiment we identified $F4/80^+$ cells in EAE mice. Our failure to find vascular derived macrophage cells may be due to the differences in age of the transgenic mice used in the different studies. Increases in $CD11b^+$ cells were first detected at approx. 4 months in *Plp1*tg heterozygous mice and their numbers increased with age (Ip et al., 2006); in contrast, we used 1–2-month-old homozygous mice as they die at approx. 2 months of age. Because the $CD11b^+$ marker is also expressed by endogenous microglial cells (Clausen et al., 2008; Santos et al., 2010; Bokhari et al., 2009), many $CD11b^+$ cells may be microglia. Other studies have shown that microglial precursors derived from embryonic stem cells co-label with Iba1 and CD11b, CD45, F4/80 (Napoli et al., 2009) and other immune cell markers, making it difficult to distinguish between resident and invasive immune cells. Since presentation of antigens by microglia to T-cells requires a period of time (Brown and Neher, 2010), a combination of both microglia and immune cells is likely present in *Plp1*tg mice, the ratios of innate to humoral cells changing as the rodents age. More important than identifying all the cell types that contribute to inflammation in the *Plp1*tgs, the molecular events that cause the inflammation and how the different cytokines modulate neuronal function need to be investigated. Importantly, the extent and type of inflammation in PMD patients needs to be examined and compared with rodents that overexpress *Plp1*.

ACKNOWLEDGEMENTS

We thank Dr Klaus Armin-Nave (Max–Planck Institute for Experimental Medicine, Göttingen, Germany) and Dr Carol Readhead (California Institute of Techology, Pasadena, CA, U.S.A.) for kindly providing *Plp1*tg mice.

FUNDING

This research was supported by the European Leukodystrophy Association [grant number 2009-041C5; to R.P.S.] and the National Institute of Neurological Disorders and Stroke of the National Institutes of Health [grant numbers NS-038236 (R.P.S.), NIH NS-22576 (I.S.), NIH NS-34741 (I.S.) and NIH NS-37766 (I.S.)].

REFERENCES

Anderson TJ, Schneider A, Barrie JA, Klugmann M, McCulloch MC, Kirkham D, Kyriakides E, Nave KA, Griffiths IR (1998) Late-onset neurodegeneration in mice with increased dosage of the proteolipid protein gene. J Comp Neurol 394:506–519.

Anderson TJ, Klugmann M, Thomson CE, Schneider A, Readhead C, Nave KA, Griffiths IR (1999) Distinct phenotypes associated with increasing dosage of the PLP gene: implications for CMT1A due to PMP22 gene duplication. Ann NY Acad Sci 883:234–246.

Baraczka K, Nékám K, Pozsonyi T, Szüts I, Ormos G (2004) Investigation of cytokine (tumor necrosis factor alpha, interleukin-6, interleukin-10) concentrations in the cerebrospinal fluid of female patients with multiple sclerosis and systemic lupus erythematosus. Eur J Neurol 11:37–42.

Barone FC, Arvin B, White RF, Miller A, Webb CL, Willette RN, Lysko PG, Feuerstein GZ (1997) Tumor necrosis factor-alpha. A mediator of focal ischemic brain injury. Stroke 28:1233–1244.

Bessert DA, Skoff RP (1999) High-resolution *in situ* hybridization and TUNEL staining with free-floating brain sections. J Histochem Cytochem 47:693–702.

Block ML, Hong JS (2005) Microglia and inflammation-mediated neurodegeneration: multiple triggers with a common mechanism. Prog Neurobiol 76:77–98.

Bo L, Vedeler CA, Nyland HI, Trapp BD, Mork SJ (2003) Subpial demyelination in the cerebral cortex of multiple sclerosis patients. J Neuropathol Exp Neurol 62:723–732.

Boison D, Büssow H, D'Urso D, Müller HW, Stoffel W (1995) Adhesive properties of proteolipid protein are responsible for the compaction of CNS myelin sheaths. J Neurosci 15:5502–5513.

Bokhari SM, Yao H, Bethel-Brown C, Fuwang P, Williams R, Dhillon NK, Hegde R, Kumar A, Buch SJ (2009) Morphine enhances Tat-induced activation in murine microglia. J Neurovirol 22:1–10.

Bradl M, Bauer J, Inomata T, Zielasek J, Nave KA, Toyka K, Lassmann H, Wekerle H (1999) Transgenic Lewis rats overexpressing the proteolipid protein gene: myelin degeneration and its effect on T cell-mediated experimental autoimmune encephalomyelitis. Acta Neuropathol 97:595–606.

Brown GC, Neher JJ (2010) Inflammatory neurodegeneration and mechanisms of microglial killing of neurons. Mol Neurobiol 41:242–247.

Campagnoni AT, Skoff RP (2001) The pathobiology of myelin mutants reveal novel biological functions of the MBP and PLP genes. Brain Pathol 11:74–91.

Cerghet M, Bessert DA, Nave KA, Skoff RP (2001) Differential expression of apoptotic markers in jimpy and in Plp overexpressors: evidence for different apoptotic pathways. J Neurocytol 30:841–855.

Clausen BH, Lambertsen KL, Babcock AA, Holm TH, Dagnaes-Hansen F, Finsen B (2008) Interleukin-1beta and tumor necrosis factor-alpha are expressed by different subsets of microglia and macrophages after ischemic stroke in mice. J Neuroinflammation 5:46.

Di Napoli MD, Schwaninger M, Cappelli R, Ceccarelli E, Di Gianfilippo G, Donati C, Emsley HC, Forconi S, Hopkins SJ, Masotti L, Muir KW, Paciucci A, Papa F, Roncacci S, Sander D, Sander K, Smith CJ, Stefanini A, Weber D (2005) Evaluation of c-reactive protein measurement for assessing the risk and prognosis in ischemic stroke: a statement for health care professionals from the CRP Pooling Project members. Stoke 36:1316–1329.

Dickson DW, Mattiace LA, Kure K, Hutchins K, Lyman WD, Brosnan CF (1991) Microglia in human disease, with an emphasis on acquired immune deficiency syndrome. Lab Invest, 64:135–156.

Dissing-Olesen L, Ladeby R, Nielsen H, Toft-Hansen H, Dalmau I, Finsen B (2007) Axonal lesion-induced microglial proliferation and microglial cluster formation in the mouse. Neurosci 149:112–122.

Duncan I, Hammang J, Trapp B (1987) Abnormal compact myelin in the myelin-deficient rat: absence of proteolipid protein correlates with a defect in the intraperiod line. Proc Natl Acad Sci USA 84:6287–6291.

Edgar JM, McCulloch MC, Montague P, Brown AM, Thilemann S, Pratola L, Gruenenfelder FI, Griffiths IR, Nave KA (2010) Demyelination and axonal preservation in a transgenic mouse model of Pelizaeus–Merzbacher disease. EMBO Mol Med 2:42–50.

Garbern JY, Cambi F, Lewis R, Shy M, Sima A, Kraft G, Vallat JM, Bosch EP, Hodes ME, Dlouhy S, Raskind W, Birt T, and Macklin W (1999) Peripheral neuropathy caused by proteolipid protein gene mutations. Ann NY Acad Sci 883:351–365.

Garbern, JY, Yool DA, Moore GJ, Wilds IB, Faulk MW, Klugmann M, Nave KA, Sistermans EA, Van der Knaap MS, Bird TD, Shy ME, Kamholz JA, Griffiths IR (2002) Patients lacking the major CNS myelin protein, proteolipid protein 1, develop length-dependent axonal degeneration in the absence of demyelination and inflammation. Brain 125:551–561.

Gonzalez-Scarano, F. and G. Baltuch (1999) Microglia as mediators of inflammatory and degenerative diseases. Annu Rev Neurosci 22:219–40.

Gorman MP, Golomb MR, Walsh LE, Hobson GM, Garbern JY, Kinkel RP, Darras BT, Urion DK, Eksioglu YZ (2007) Steroid-responsive neurologic relapses in a child with a proteolipid protein-1 mutation. Neurology 68:1305–1307.

Gow A, Southwood CM, Lazzarini RA (1998) Disrupted proteolipid protein trafficking results in oligodendrocyte apoptosis in an animal model of Pelizaeus–Merzbacher disease. J Cell Biol 140:925–934.

Graeber M, López-Redondo F, Ikoma E, Ishikawa M, Imai Y, Nakajima K, Krutzberg GW, Kohsaka S (1998) The microglia/macrophage response in the neonatal rat facial nucleus following axotomy. Brain Res 813:241–253.

Gray E, Thomas T, Betmouni S, Scolding N, Love S (2008). Elevated activity and microglial expression of myeloperoxidase in demyelinated cerebral cortex in multiple sclerosis. Brain Pathology 18:86–95

Griffiths I, Klugmann M, Anderson T, Thomson C, Vouyiouklis D, Nave KA (1998) Current concepts of PLP and its role in the nervous system. Microsc Res Tech 41:344–358.

Gudz TI, Schneider TE, Haas TA, Macklin WB (2002) Myelin proteolipid protein forms a complex with integrins and may participate in integrin receptor signaling in oligodendrocytes. J Neurosci 22:7398–7407.

Gyoneva S, Orr AG, Traynelis SF (2009) Differential regulation of microglial motility by ATP/ADP and adenosine. Parkinsonism Relat Disord 15:S195-S199.

Hodes ME, Pratt VM, Dlouhy SR (1993) The genetics of Pelizaeus–Merzbacher disease. Dev Neurosci 15:383–394.

Hüttemann M, Zhang Z, Mullins C, Bessert D, Lee I, Nave KA, Appikatla S, Skoff RP (2009) Different proteolipid protein mutants exhibit unique metabolic defects. ASN Neuro 1:e00014

Imai Y, Ibata I, Ito D, Ohsawa K, Kohsaka S (1996) A novel gene iba1 in the major histocompatibility complex class III region encoding an EF hand protein expressed in a monocytic lineage. Biochem Biophys Res Commun 224:855–862.

Ip CW, Kroner A, Bendszus M, Leder C, Kobsar I, Fischer S, Wiendl H, Nave KA, Martini R (2006) Immune cells contribute to myelin degeneration and axonopathic changes in mice overexpressing proteolipid protein in oligodendrocytes. Neurobiol Dis 26:8206–8216.

Ito D, Imai Y, Ohsawa K, Nakajima K, Fukuuchi Y, Kohsaka S (1998) Microglia-specific localisation of a novel calcium binding protein, Iba1. Mol Brain Res 57:1–9.

Kagawa T, Ikenaka K, Inoue Y, Kuriyama S, Tsujii T, Nakao J, Nakajima K, Aruga J, Okano H, Mikoshiba K (1994) Glial cell degeneration and hypomyelination caused by overexpression of myelin proteolipid protein gene. Neuron 13:427–442.

Kawashita E, Tsuji D, Kawashima N, Nakayama K, Matsuno H, Itoh K (2009) Abnormal production of macrophage inflammatory protein-1alpha by microglial cell lines derived from neonatal brains of Sandhoff disease model mice. J Neurochem 109:1215–1224.

Knapp PE (1996) Proteolipid protein: is it more than just a structural component of myelin? Dev Neurosci 18:297–308.

Knapp PE, Booth CS, Skoff RP (1993) The pH of jimpy glia is increased: intracellular measurements using fluorescent laser cytometry. Int J Dev Neurosci 11:215–226.

Knerlich-Lukoschus F, von der Ropp-Brenner B, Lucius R, Mehdorn HM, Held-Feindt J (2010) Chemokine expression in the white matter spinal cord precursor niche after force-defined spinal cord contusion injuries in adult rats. Glia 58:916–931.

Kreutzberg GW (1996) Microglia: a sensor for pathological events in the CNS. Trends Neurosci 19:312–318.

Kutzelnigg A, Lucchinetti CF, Stadelmann C, Bruck W, Rauschka H, Bergmann M (2005) Cortical demyelination and diffuse white matter injury in multiple sclerosis. Brain 128:2705–2712.

Lambert C, Ase AR, Séguéla P, Antel JP (2010) Distinct migratory and cytokine responses of human microglia and macrophages to ATP. Brain Behav Immun, doi:10.1016/j.bbi.2010.02.010.

Macklin WB, Campagnoni CW, Deininger PL, Gardinier MV (1987) Structure and expression of the mouse myelin proteolipid protein gene. J Neurosci Res 18:383–394.

Macklin WB, Gardinier MV, Obeso ZO, King KD, Wight PA (1991) Mutations in the myelin proteolipid protein gene alter oligodendrocyte gene expression in jimpy and jimpy msd mice. J Neurochem 56:163–171.

Mastronardi FG, Ackerley CA, Arsenault L, Roots BI, Moscarello MA (1993) Demyelination in a transgenic mouse: a model for multiple sclerosis. J Neurosci Res 36:315–324.

Matsumoto Y, Ohmori K, Fujiwara M (1992) Microglial and astroglial reactions to inflammatory lesions of experimental autoimmune encephalomyelitis in the rat central nervous system. J Neuroimmunol 37:23–33.

McGeer PL Kawamata T, Walker DG, Akiyama H, Tooyama I, McGeer EG (1993) Microglia in degenerative neurological disease. Glia 7:84–92.

Monif M, Reid CA, Powell KL, Smart ML, Williams DA (2009) The P2X7 receptor drives microglial activation and proliferation: a trophic role for P2X7R pore. J Neurosci 29:3781–3791.

Nadon NL, West M (1998) Myelin proteolipid protein: function in myelin structure is distinct from its role in oligodendrocyte development. Dev Neurosci 20:533–539.

Napoli I, Kierdorf K, Neumann H (2009) Microglial precursors derived from mouse embryonic stem cells. Glia 57:1660–1671.

Navikas V, Link H (1996) Review: cytokines and the pathogenesis of multiple sclerosis. J Neurosci Res 45:322–333.

Peterson JW, Bo L, Mork S, Chang A, Trapp BD (2001) Transected neurites, apoptotic neurons, and reduced inflammation in cortical multiple sclerosis lesions. Ann Neurol 50:389–400.

Puthussery T, Fletcher E (2009) Extracellular ATP induces retinal photoreceptor apoptosis through activation of purinoceptors in rodents. J Comp Neurol 513:430–440.

Readhead C, Schneider A, Griffiths I, Nave KA (1994) Premature arrest of myelinformation in transgenic mice with increased proteolipid protein gene dosage. Neuron 12:583–595.

Regis S, Grossi S, Lualdi S, Biancheri R, Filocamo M (2005) Diagnosis of Pelizaeus–Merzbacher disease: detection of proteolipid protein gene copy number by real-time PCR. Neurogenetics 6:73–78.

Santos AM, Martin-Oliva D, Ferrer-Martin RM, Tassi M, Calvente R, Sierra A, Carrasco MC, Marin-Teva JL, Navascués J, Cuadros MA (2010) Microglial response to light-induced photoreceptor degeneration in the mouse retina. J Comp Neurol 518:477–492.

Skoff RP (1975) The fine structure of pulse labeled (3-H-thymidine cells) in degenerating rat optic nerve. J Comp Neurol 161:595–611.

Skoff RP (1976) Myelin deficit in the Jimpy mouse may be due to cellular abnormalities in astroglia. Nature 264:560–562.

Skoff RP, Knapp PE (1990) Expression of the jimpy phenotype in relation to proteolipid protein appearance. Ann NY Acad Sci 605:122–134.

Skoff RP, Bessert DA, Cerghet M, Franklin MJ, Rout UK, Nave KA, Carlock L, Ghandour MS, Armant DR (2004a) The myelin proteolipid protein gene modulates apoptosis in neural and non-neural tissues. Cell Death Diff 11:1247–1257

Skoff RP, Saluja I, Bessert D, Yang X (2004b) Analyses of proteolipid protein mutants show levels of proteolipid protein regulate oligodendrocyte number and cell death *in vitro* and *in vivo*. Neurochem Res 29:2095–2103.

Stoffel W, Giersiefen H, Hillen H, Schroeder W, Tunggal B (1985) Amino-acid sequence of human and bovine brain myelin proteolipid protein (lipophilin) is completely conserved. Biol Chem Hoppe-Seyler 366:627–635.

Szalai AJ, Nataf S, Hu XZ, Barnum SR (2002) Experimental allergic encephalomyelitis is inhibited in transgenic mice expressing human C-reactive protein. J Immunol 168:5792–5797.

Thomas WE (1992) Brain macrophages: evaluation of microglia and their functions. Brain Res Rev 17:61–74.

Tonchev AB, Yamashima T, Zhao L, Okano H (2003) Differential proliferative response in the postischemic hippocampus, temporal cortex, and olfactory bulb of young adult macaque monkeys. Glia 42:209–224.

Vela J, Dalmau I, Acrín L, González B, Castellano B (1995) Microglial cell reaction in the gray and white matter in spinal cords from jimpy mice. An enzyme histochemical study at the light electron microscope level. Brain Res 694:287–298.

Vela J, Dalmau I, González, B, Castellano B (1996) Understanding glial abnormalities associated with myelin deficiency in the jimpy mutant mouse. Brain Res 712:134–142.

Vladic A, Horvat G, Vukadin S, Sucic Z, Simaga S (2002) Cerebrospinal fluid and serum protein levels of tumor necrosis factor-alpha (TNF-alpha), interleukin-6 (IL-6) and soluble interleukin-6 receptor (sIL-6-R gp80) in multiple sclerosis patients. Cytokine 20:86–89.

Vercellino M, Plano F, Votta B, Mutani R, Giordana MT, Cavalla P (2005) Grey matter pathology in multiple sclerosis. J Neuropathol Exp Neurol 64:1101–1107.

Wojtera M, Sikorska B, Sobow T, Liberski PP (2005) Microglial cells in neurodegenerative disorders. Folia Neuropathol 43:311–321.

Yamada M, Ohsawa K, Imai Y, Kohsaka S, Kamitori S (2006) X-ray structures of the microglia/macrophage-specific protein Iba1 from human and mouse demonstrate novel molecular conformation change induced by calcium binding. J Mol Biol 364:449–457.

Yang X, Skoff RP (1997) Proteolipid protein regulates the survival and differentiation of oligodendrocytes. J Neurosci 17:2056–2070.

Zhang F, Vadakkan K, Kim S, Wu L, Shang Y, Zhuo M (2008) Selective activation of microglia in spinal cord but not higher cortical regions following nerve injury in adult mouse. Mol Pain 4:15.

Received 21 May 2010/11 August 2010; accepted 19 August 2010

Published as Immediate Publication 23 August 2010, doi 10.1042/AN20100016